The College at Brockport: State University of New York
Digital Commons @Brockport

Earth Sciences Faculty Publications | Department of the Earth Sciences

6-2006

The Role of Sublimational Cooling in a Late-Season Midwestern Snow Event

Patrick S. Market
University of Missouri - Columbia

Ronald W. Przybylinksi
National Weather Service

Scott M. Rochette
The College at Brockport, rochette@esc.brockport.edu

Follow this and additional works at: https://digitalcommons.brockport.edu/esc_facpub

 Part of the Earth Sciences Commons

Repository Citation

Market, Patrick S.; Przybylinksi, Ronald W.; and Rochette, Scott M., "The Role of Sublimational Cooling in a Late-Season Midwestern Snow Event" (2006). *Earth Sciences Faculty Publications*. 3.
https://digitalcommons.brockport.edu/esc_facpub/3

Citation/Publisher Attribution:
Market, P. S., Przybylinski, R. W., and Rochette, S. M., 2006, The Role of Sublimational Cooling in a Late-season Midwestern Snow Event, *Wea. Forecasting*, 21, 364-382. Available on publisher's site at http://journals.ametsoc.org/doi/abs/10.1175/WAF919.1.

This Article is brought to you for free and open access by the Department of the Earth Sciences at Digital Commons @Brockport. It has been accepted for inclusion in Earth Sciences Faculty Publications by an authorized administrator of Digital Commons @Brockport. For more information, please contact kmyers@brockport.edu.

The Role of Sublimational Cooling in a Late-Season Midwestern Snow Event

PATRICK S. MARKET

Department of Soil, Environmental, and Atmospheric Sciences, University of Missouri—Columbia, Columbia, Missouri

RONALD W. PRZYBYLINSKI

National Weather Service Forecast Office, Weldon Spring, Missouri

SCOTT M. ROCHETTE

Department of the Earth Sciences, State University of New York—College at Brockport, Brockport, New York

(Manuscript received 23 July 2004, in final form 25 September 2005)

ABSTRACT

Analysis is provided of a surprise late-season snow event over eastern Missouri and western Illinois. While snow totals failed to exceed 15 cm (6 in.) at any single location, the system was noteworthy because of the poor performance of public, private, and media forecasts in anticipating the event. Using observed data and a successful simulation with a mesoscale numerical model, the event is scrutinized to determine the forcing mechanisms for the precipitation over a small area. A region of enhanced frontogenesis is diagnosed over the region both in the observed data as well as the model output. That the precipitation fell as snow is shown to be the result of a dry layer of air between the surface and the cloud base that saturated and cooled due largely to snow sublimation–evaporation in just a few hours to permit the fall of snow uninhibited from the cloud base to the ground.

1. Introduction

The morning of 10 April 1997 featured an unanticipated, late-season snow event over eastern Missouri and western Illinois (Fig. 1). Although storm total snow amounts were small (less than 15 cm), the general lack of warning snarled the morning commute, especially around metropolitan St. Louis, and the inclement weather forced a rare postponement of opening day for the St. Louis Cardinals baseball season. In the wake of the event, an examination of historical records showed that there were only three other events that occurred later in the season with greater snowfall totals. To the best of the authors' knowledge, forecasts (public, private, and media) from the day prior to the event discussed the possibility of rain (at worst), but none included a mention of snowfall in the urban areas of east-central Missouri or western Illinois; anecdotally, all three authors prepared forecasts for the region on 09 April 1997.

Situated in a relatively benign synoptic setting, this snow event was driven largely by low-level warm advection and frontogenesis and the presence of an initially dry near-surface layer with wet-bulb and ice-bulb temperatures near 0°C. The dry boundary layer was responsible for allowing snowfall to reach the surface, instead of the rain that had been mentioned in many forecasts. Sublimation of snow or "wet-bulbing" is a widely accepted (yet little studied) process for cooling and moistening a deep layer over a short period. Indeed, melting has been identified by a number of investigators as a common culprit for unanticipated snow events.

McGuire and Penn (1953) and Wexler et al. (1954) discuss the role of melting snow that led to the Boston snow event of 13 April 1953. This late-season event forced a delay of opening day for the Boston Red Sox baseball season, similar to that suffered by the Cardinals as noted previously. Melting of snow in the lower troposphere and the subsequent cooling helped to

Corresponding author address: Patrick S. Market, Dept. of Soil, Environmental, and Atmospheric Sciences, University of Missouri—Columbia, 302 Anheuser-Busch Natural Resources Bldg., Columbia, MO 65211-7250.
E-mail: marketp@missouri.edu

© 2006 American Meteorological Society

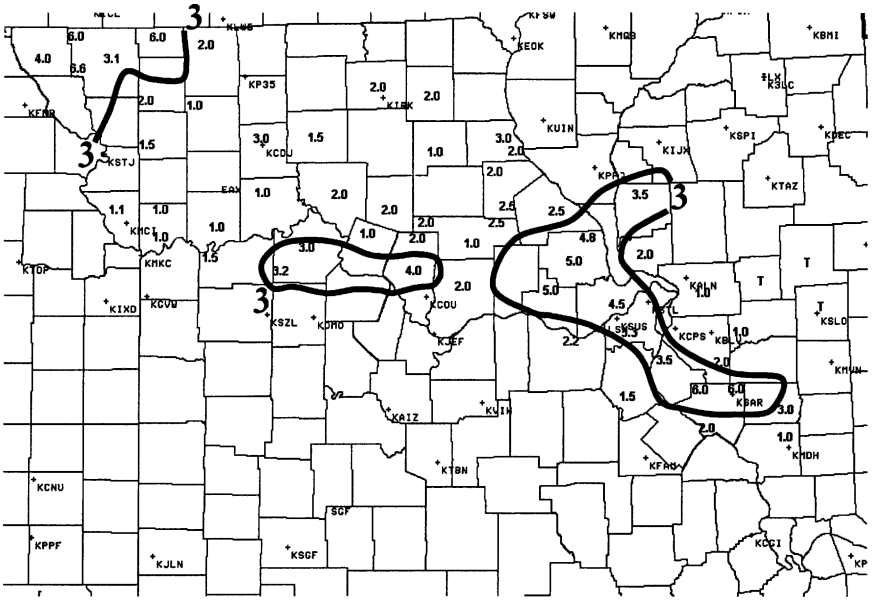

FIG. 1. Storm total snowfall values plotted in in. and tenths, and contoured (solid) for those areas where 3 in. (7.6 cm) or more snow fell.

lower surface temperatures by 4.5°C and the freezing level more than 1800 m over a period of 1 h. Heavy rain rapidly changed to sleet and then to large, wet snowflakes, resulting in snow depths from 6 to 10 cm (2.4 to 4.0 in.) over the Boston metropolitan area.

Lumb (1961) notes that under moist-adiabatic conditions, moderate snow will survive to depths where the wet-bulb temperature T_w ranges from 1.5° to 3.5°C, and during heavy precipitation events may remain snow at T_w values approaching 4.5°C. Numerical model simulations performed by Hansson (1999) underscore the importance of subcloud T_w, in which experiments with the melting layer set as $T_w = 0$°C (instead of $T = 0$°C) resulted in a later or nonexistent snow-to-rain transformation.

Gedzelman and Lewis (1990) discuss the idea of "warm" snowstorms, those that occur during the early fall or late spring months under conditions that would

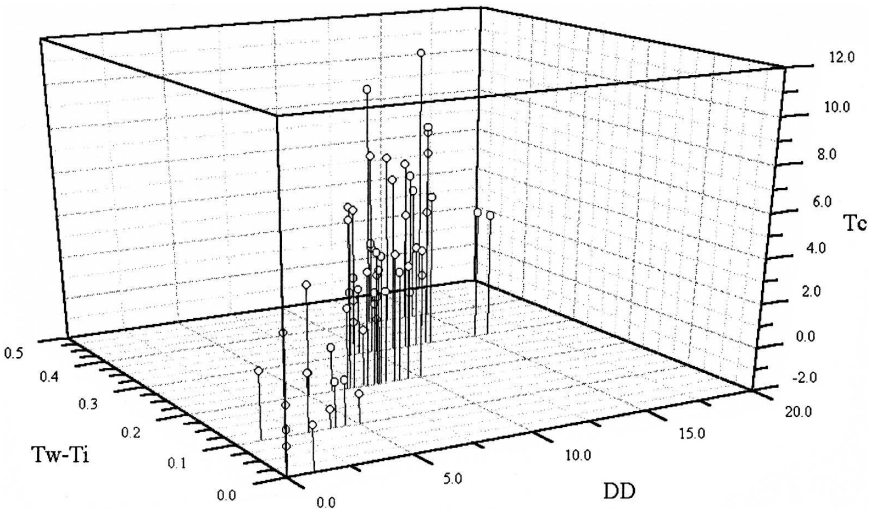

FIG. 2. A plot of dewpoint depression DD (x axis) vs $T_w - T_i$ (y axis) vs the ambient temperature T_c (z axis) for 69 randomly selected surface stations across MO and IL between 0000 and 1200 UTC 10 Apr 1997. All values are in °C.

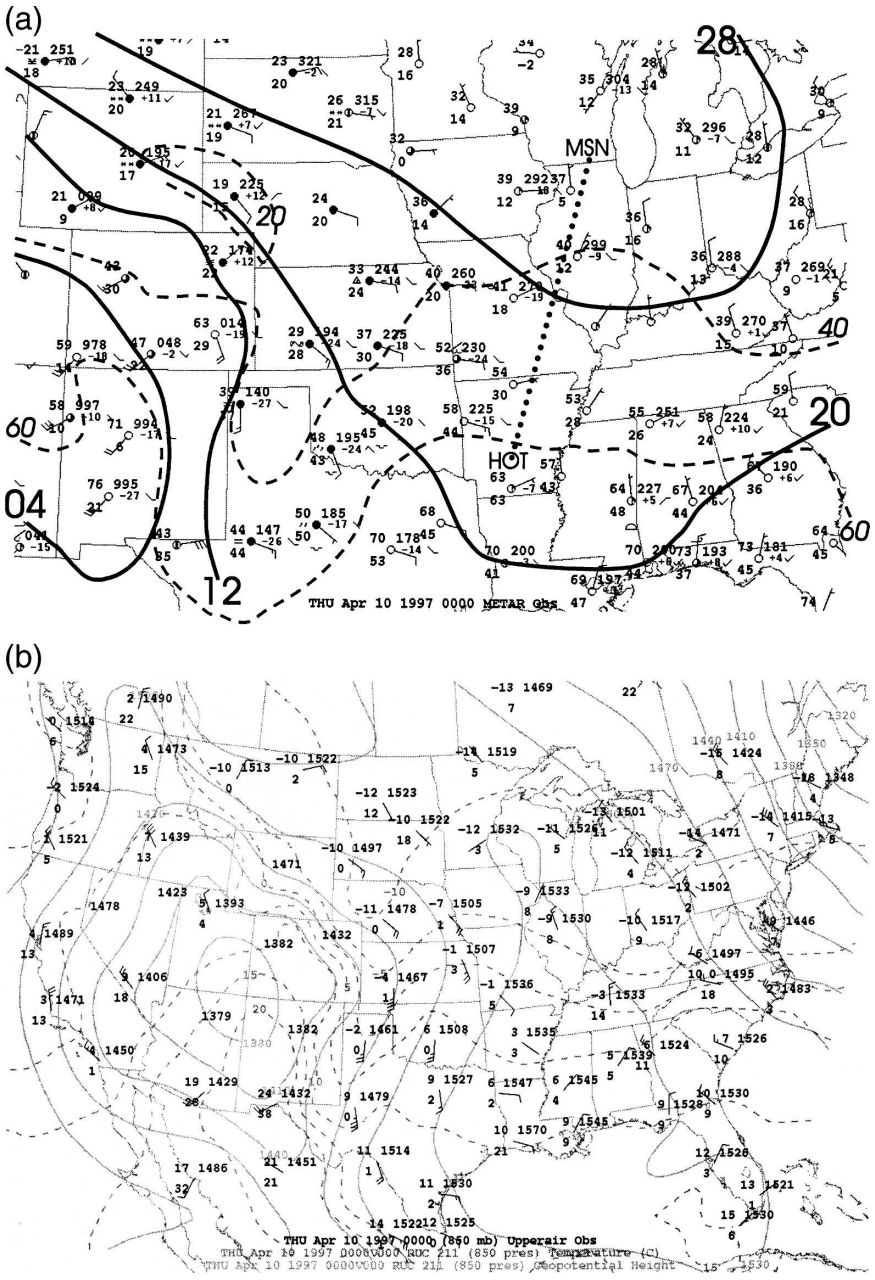

FIG. 3. Analyses valid at 0000 UTC 10 Apr 1997. (a) Surface analysis with standard station models, with subjectively analyzed isobars (solid; every 8 mb) and isotherms (dashed, every 20°F). Surface stations shown are a subset of those used for the subjective analysis. The dotted line represents the cross section shown in Figs. 14 and 15. (b) The 850-mb station plots with Rapid Update Cycle (RUC) initial field analyses of geopotential height (solid; every 30 gpm) and temperature (dashed; every 5°C). (c) The 700-mb frontogenesis [every 0.25 K (100 km)$^{-1}$ (3 h)$^{-1}$] derived from the RUC model initial fields. (d) The 500-mb station plots with RUC initial field analyses of geopotential height (solid, every 60 gpm) and temperature (dashed; every 5°C). (e) Skew T–log$p$ analysis for observed sounding at Lincoln, IL.

appear too warm to support snow. They cite three significant examples of major snow events that should not have been: 1) 3–4 October 1987, during which up to 50 cm (20 in.) of snow fell over eastern New York and western New England; 2) 26–27 April 1988, an event that brought a record 35-cm (14 in.) snowfall to Rochester, Minnesota; and 3) 9 May 1977, a very late event that produced up to 65 cm (26 in.) of snow across parts

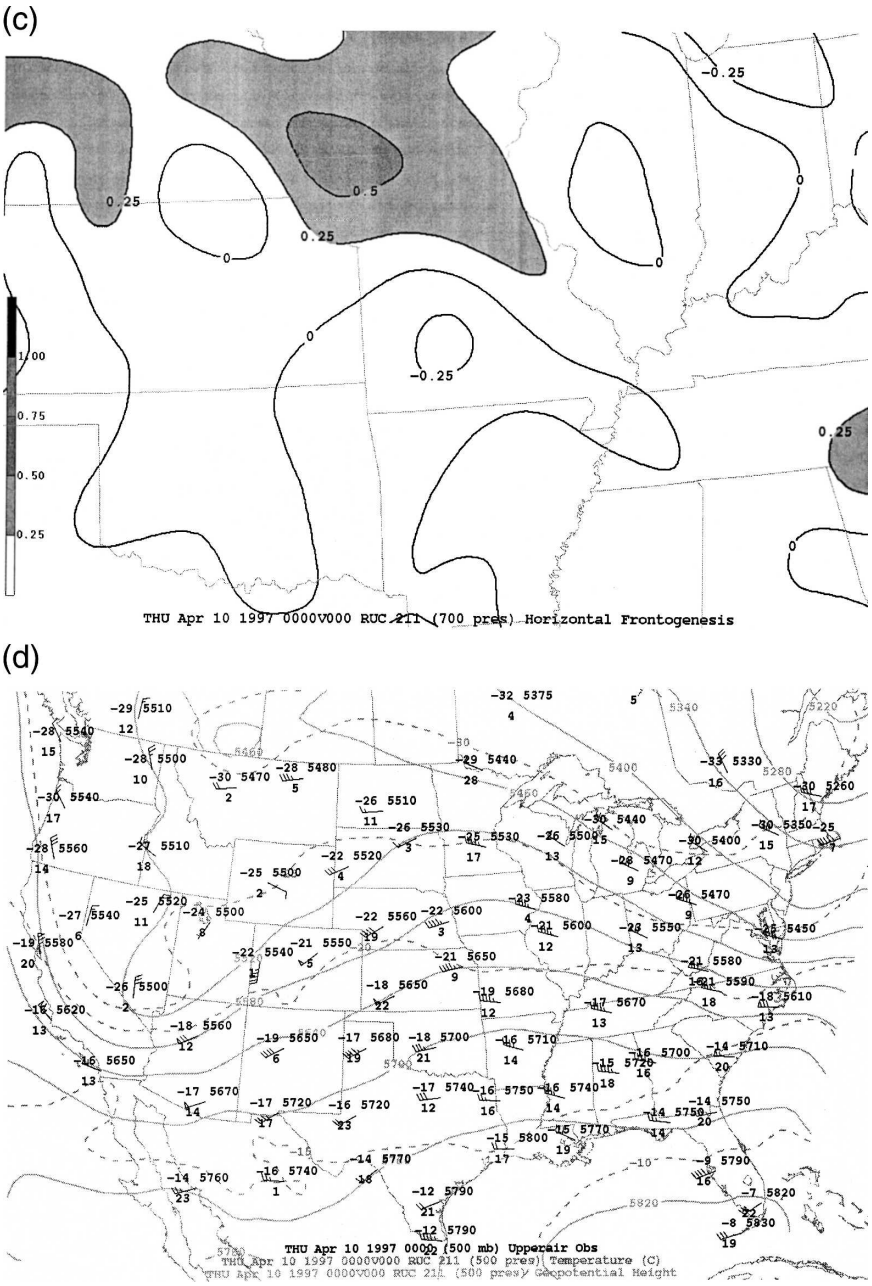

FIG. 3. (*Continued*)

of the lower Hudson River Valley and southern New England. Snowfall amounts from 9 May 1977 were strongly correlated to elevation, with minimal accumulations for locations near sea level [e.g., 3.2 cm (1.3 in.) at Hartford, Connecticut].

Modeling studies by Szeto and Stewart (1997) illustrate the effect of melting snow on surface frontogenesis. They found that baroclinicity is locally enhanced and frontogenesis is accelerated through finescale perturbations of the thermal and kinematic fields in the frontal zone at the level where melting snow exists. They further note that these effects should be strongest when the melting layer is near the surface.

Kain et al. (2000) cite a "surprise" heavy snow event that occurred in east-central Tennessee and its environs on 3–4 February 1998, in which more than 30 cm (12 in.) of snow fell in some locations, which was preceded by locally heavy rainfall. They conclude that the dominant factor in the unexpected changeover to snow was cooling due to melting snowflakes. From this study they

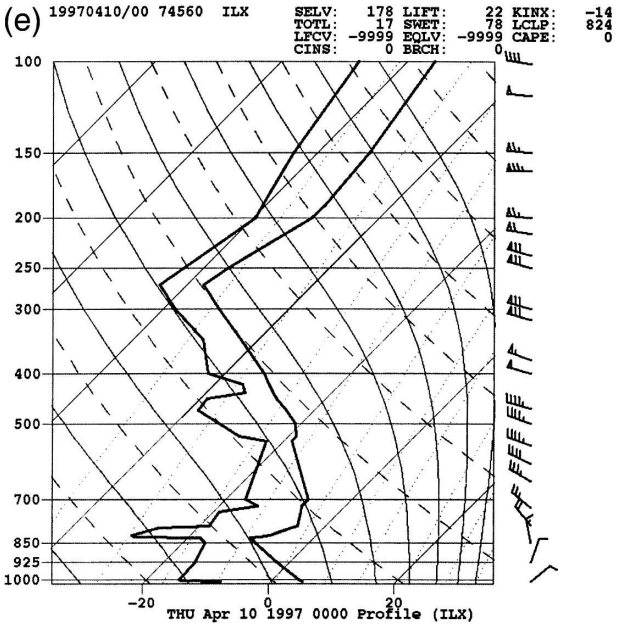

FIG. 3. (*Continued*)

developed three criteria that, when met, should alert forecasters to the importance of the melting effect: 1) weak low-level temperature advection; 2) steady rainfall of moderate to heavy intensity, expected to persist for several hours; and 3) surface temperatures within several degrees of 0°C at the onset of the event.

Unlike many previous works, this study seeks to address cooling by both melting *and* sublimation of snowflakes. As such, a brief note on method is necessary. This paper makes use of the ice-bulb temperature T_i, where appropriate. As we are dealing with an environment where both melting and evaporation occurred, we must account for both kinds of latent heat that attend these processes. It is well established (e.g., Hess 1959) that the difference between the latent heat of evaporation and the latent heat of sublimation is small, with the former constituting ~88% of the latter; thus, $T_w > T_i$. A sample of calculations from surface stations in the 12 h leading up to this event revealed a mean difference between T_w and T_i of 0.2°C, with a maximum value of 0.5°C (Fig. 2), the latter being a case with a temperature of 10°C and a dewpoint depression of 17°C. Yet, sublimation does permit greater cooling, and it will be accounted for as needed.

This paper will demonstrate the importance of both frontogenesis in forcing ascent with this event and the dry lower-tropospheric air for allowing sublimation of snow and the creation of a subfreezing layer all the way to the surface in a late-season event; it is the latter issue that led to widespread error in the forecasting community with this event. Section 2 provides a brief synoptic overview of the event. Section 3 provides a mesoscale analysis of the precipitation band evolution with an emphasis on profiler and Weather Surveillance Radar-1988 Doppler (WSR-88D) observations. A model perspective of the event is detailed in section 4, along with a brief description of the model architecture employed. In section 5, we offer some concluding remarks.

2. Synopsis

At 0000 UTC 10 April 1997 (all observed and modeled times are hereafter associated with this date unless otherwise indicated), a dry easterly surface flow dominates eastern Missouri, generated by an elongated ridge of high pressure east of the state (Fig. 3a). Overnight, winds at St. Louis, Missouri (STL; Table 1), veer and become southeasterly by the end of the snow event. Although some moistening of the boundary layer occurred, dewpoint depressions consistently permit a surface T_w very near 0°C. An analysis of the 850-mb level (Fig. 3b) reveals the axis of a sharp anticyclonic ridge centered over the region of interest. This is highlighted by the moist, southeasterly flow over the western half of Missouri contrasting with the dry, northerly flow over the rest of Missouri as well as western Illinois. An advection couplet is also suggested, with warm air advection present south of the east–west-oriented trough over northwestern Missouri and weak cold advection diagnosed over the southeastern portion of the state.

An objective analysis of the 700-mb level reveals frontogenesis over most of Missouri (Fig. 3c), with the strongest values over the northern and eastern portions of the state. The expression for frontogenesis is given by Petterssen (1956) as

$$\mathcal{F} = \frac{|\nabla\theta|}{2}\{\text{def}[\cos(2\beta)] - \text{div}\}, \quad (1)$$

where β is the angle between the axis of dilatation of the total deformation field and the isentrope (θ) field and def (div) is the resultant deformation (divergence) of the wind field. In addition, $\mathcal{F}$ can be altered by changes in the magnitude or orientation of the thermal gradient vector and by the orientation of the flow field; resultant deformation is always a positive value, and the sign of the larger term is thus controlled ultimately by β. Spatial changes in the magnitude of the flow field (divergence) also contribute to frontogenesis.

The 500-mb flow pattern appears quiescent over the Midwest (Fig. 3d). A cyclonic circulation off the Canadian Maritimes and a deepening trough over the desert Southwest have a ridge in between, the axis of which

TABLE 1. Selected surface observations from KSTL on 10 Apr 1997. Present weather (Wx), ceiling (CIG), and remarks follow the METAR coding convention.

Time (UTC)	Wind (°/kt)	Visibility (mi.)	Wx	CIG	T (°C)	T_d (°C)	Altimeter (in Hg)	Remarks
0255	110/9	10	—	SCT250	4	−7	30.37	—
0855	100/7	10	—	OVC070	4	−6	30.34	—
0955	110/4	10	—	BKN047	4	−5	30.37	VIRGA
1020	120/10G16	2.5	−SN	OVC035	3	−4	30.40	SNB19
1055	110/8	0.75	−SN	BKN005	0	0	30.39	—
1155	110/10	0.5	SN	OVC004	0	0	30.40	SNINCR1/1
1255	120/13	0.5	SN	OVC004	0	0	30.40	SNINCR1/2
1355	130/14	0.5	SN	OVC007	0	0	30.38	—
1455	120/15	1	−SN	BKN004	0	0	30.34	SNINCR1/4

lies along and just west of Missouri at 0000 UTC 10 April 1997. The veering (backing) winds with height at Springfield, Missouri (Lincoln, Illinois), further demonstrate the warm (cold) advection discussed earlier for 850 mb.

The 0000 UTC sounding for Lincoln, Illinois (ILX), reveals a dry, well-mixed boundary layer, capped by a subsidence inversion associated with the anticyclone (Fig. 3e). This sounding is particularly appropriate to this case, as it is upstream of STL in a boundary layer flow sense. Being a sunset sounding east of the ridge axis with a T_w profile that is everywhere less than freezing, the lapse rate was destined to cool and stabilize near the surface. The backing wind profile near the surface is further evidence of the weak cold advection suggested in Fig. 3b.

The surface field at 1200 UTC 10 April 1997 (Fig. 4a) reveals evidence of an elongated warm frontal zone. Precipitation is also reported over a far broader region (parts of Missouri and Kansas) north of the frontal zone. Note, however, that eastern Missouri and western Illinois are well within the cold air and that the flow persists with a strong easterly component. At 850 mb (Fig. 4b), the ridge axis was well east of the Mississippi River and deamplified. Nevertheless, warm air advection and dewpoint depressions of <5°C cover most of Missouri. Yet, the 700-mb frontogenesis analysis (Fig. 4c) reveals a weakly frontolytic environment over STL. As we will see, the more significant frontogenetical forcing existed in the midtroposphere over STL prior to 1200 UTC and for only a short time.

At 500 mb, the trough over the Rockies had deepened by as much as 70 gpm over Arizona, while the ridge over the central United States was largely in the same location (Fig. 4d). Evidence for this gradual motion is found in height changes of 10 gpm or less across Arkansas, Missouri, Kansas, and Nebraska. A weak short-wave trough is also found cresting the top of the ridge, highlighted by the lack of height tendencies at Topeka, Kansas, and Springfield, Missouri, over the preceding 12-h period. Even at this level, dewpoint depressions are 5°C or less over the northeastern half of Missouri.

At 1200 UTC, the ILX sounding profiles (Fig. 4e) of ambient, wet-bulb, and dewpoint temperatures were everywhere below freezing, with the flow in the lowest ~1000 m having an easterly component. While significant moistening and warming has occurred above 900 mb, the layer beneath remains unsaturated. Moreover, the flow in this lowest layer is 5 m s^{-1} or less, suggesting weak boundary layer advections.

3. Observed features

a. WSR-88D radar observations

WSR-88D observations from the National Weather Service in St. Louis, Missouri (KLSX), are shown from 0901 through 1200 UTC, during the period when precipitation begins over much of east-central Missouri and southwestern Illinois. At 0901 UTC reflectivity data at 0.5° elevation angle show a mesoscale precipitation band extending from Kirksville, Missouri (KIRK), to 50 km southeast of Lambert–St. Louis International Airport (KSTL). The length of the band is over 250 km, while the width varies from 30 to 40 km (Fig. 5). Reflectivity values generally range from 20 to 30 dBZ, with an area of 35–40 dBZ detected 15 km southwest of KLSX and embedded within the larger mesoscale band. The mesoscale precipitation band observed at this time is similar in size and time duration to the mesoscale snowbands observed by Nicosia and Grumm (1999) and recent climatological cold-season banded precipitation over the northeast United States (Novak et al. 2002). Their studies assumed that for a precipitation structure to be classified as a mesoscale band, it must meet the following minimum criteria: (a) 250-km length, (b) 100-km width, (c) 30-dBZ reflectiv-

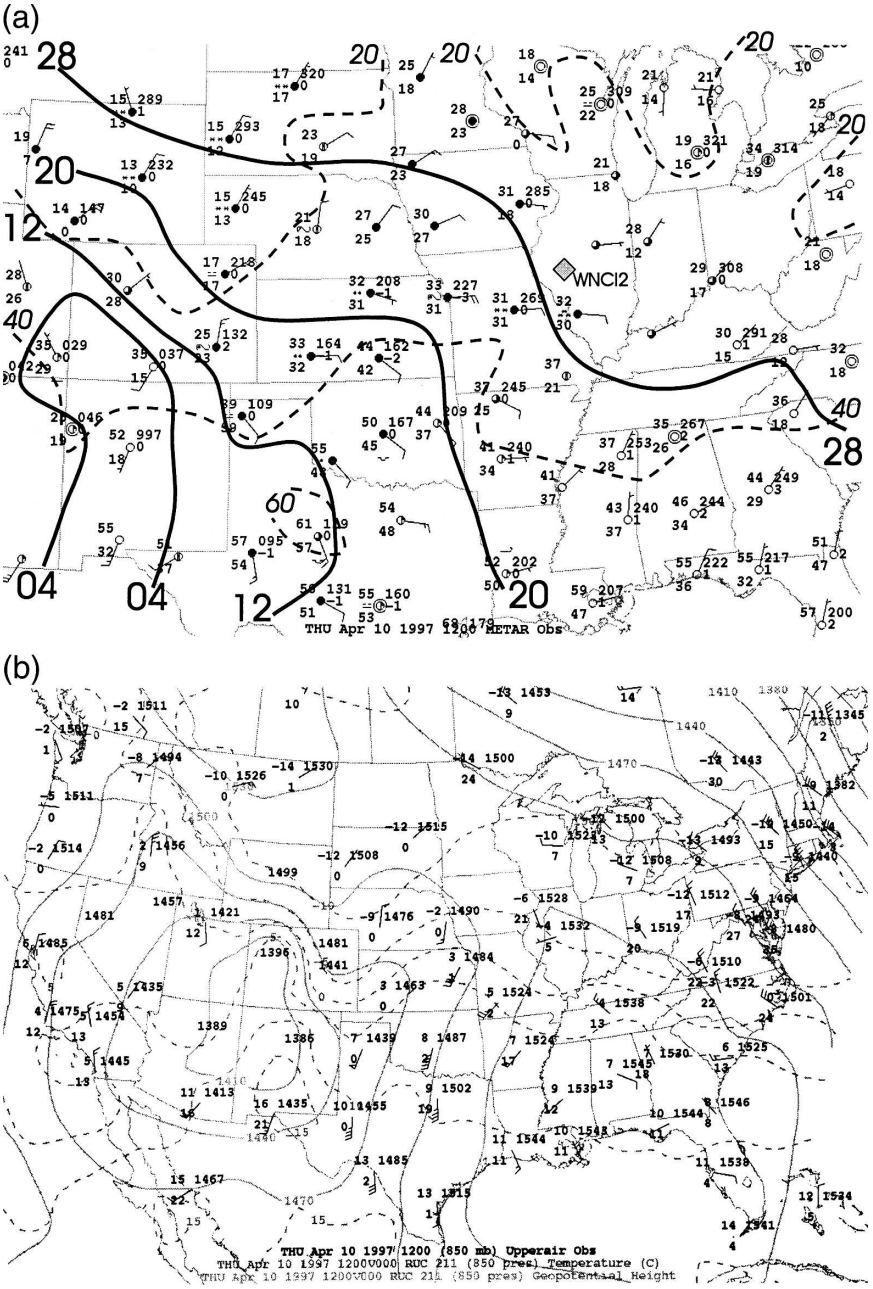

FIG. 4. Analyses valid at 1200 UTC 10 Apr 1997. (a) Surface analysis with standard station models, with subjectively analyzed isobars (solid; every 8 mb) and isotherms (dashed, every 20°F). Surface stations shown are a subset of those used for the subjective analysis. The diamond labeled WNCI2 denotes the profiler at Winchester, IL, for which data are shown in Fig. 9. (b) The 850-mb station plots with RUC initial field analyses of geopotential height (solid; every 30 gpm), and temperature (dashed; every 5°C). (c) The 700-mb frontogenesis [every 0.25 K $(100\ \text{km})^{-1}\ (3\ \text{h})^{-1}$] derived from the RUC model initial fields. (d) The 500-mb station plots with RUC initial field analyses of geopotential height (solid, every 60 gpm) and temperature (dashed; every 5°C). (e) The skew T–log$p$ analysis for the observed sounding at Lincoln, IL.

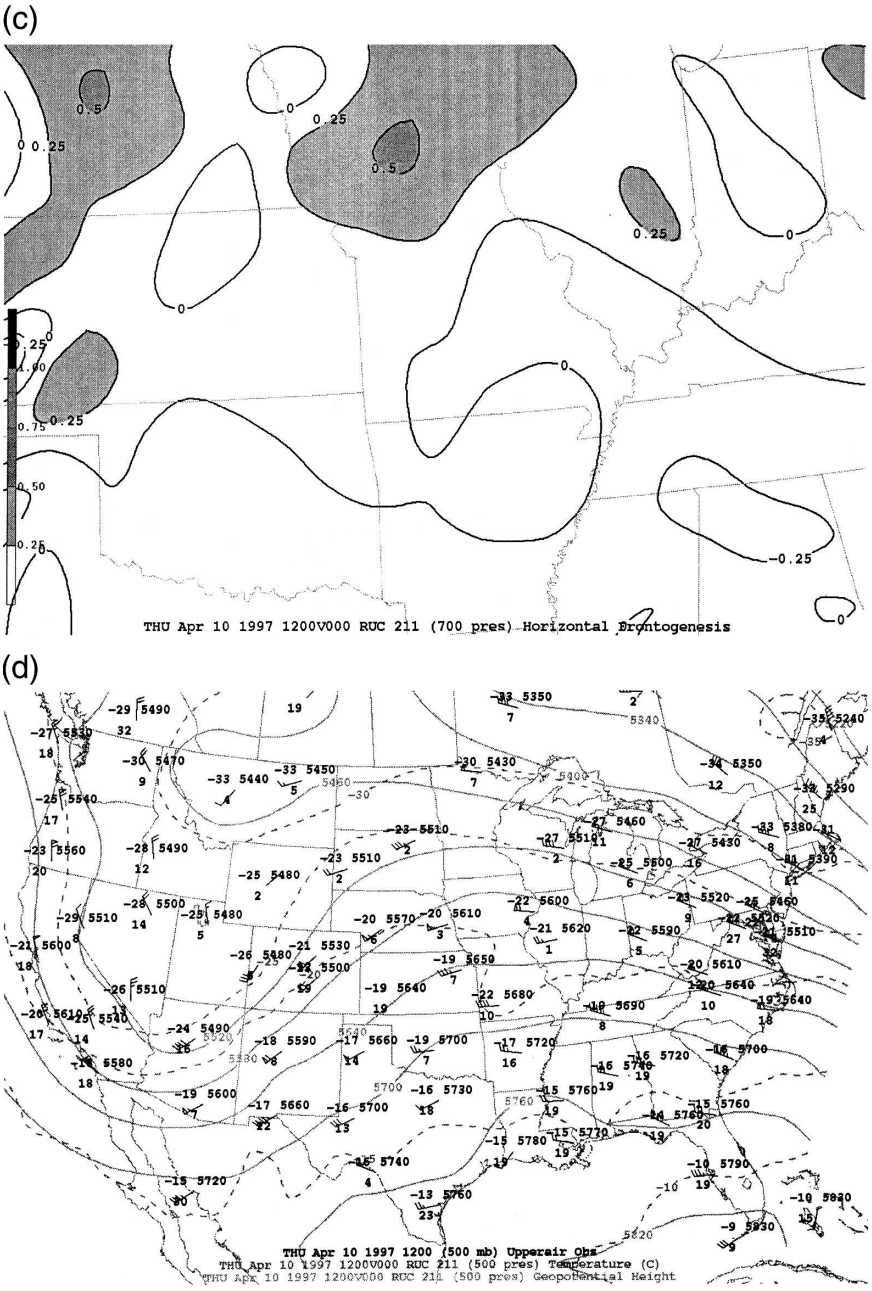

FIG. 4. (*Continued*)

ity values, and (d) 2-h minimum duration. The larger mesoscale band observed at this time shows a distinct reflectivity gradient along its leading edge from just southeast of KLSX through southern Illinois. The presence of the strong reflectivity gradient and absence of precipitation immediately to the northeast suggest that subsidence flow and very dry air were present immediately northeast of the mesoscale precipitation band. In contrast, the southern and southwest parts of the precipitation area reveal a broken area of small convective cells across parts of south-central and central Missouri. Reflectivity values of 35–40 dBZ are detected within a few of these smaller cells, and some are merging northeastward into the larger mesoscale band.

One hour later (1000 UTC), the larger mesoscale band extends from 170 km northwest to 150 km southeast of KLSX (Fig. 6). The width of the mesoscale band expands in size from 0900 UTC, varying from 50 to 80 km.

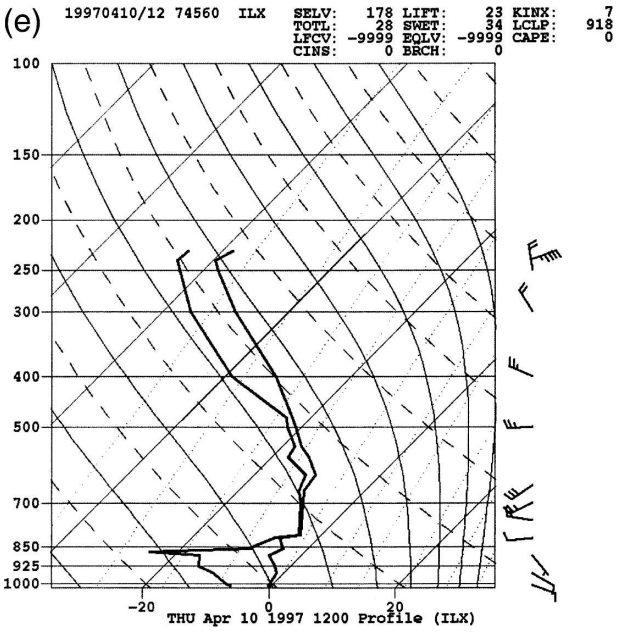

FIG. 4. (*Continued*)

Pockets of higher reflectivity within the band reach 35–40 dBZ, suggesting the presence of relatively high snowfall rates. Snow starts to fall over western and southern parts of the St. Louis metropolitan area. Smaller mesoscale precipitation bands, having an overall length of 100–120 km, also form over parts of far northeastern Missouri and west-central Illinois at this time. These smaller bands also show a similar northwest–southeast orientation to the larger band.

Approximately 1 h later (1059 UTC), the overall structure of the large mesoscale band further expands in width and length (Fig. 7). The mesoscale band continues to maintain its overall structure as it extends over 400 km in length across northeast Missouri through far southern Illinois. Pockets of higher reflectivity reaching 45 dBZ are noted immediately south of KLSX across the southern part of the St. Louis metropolitan area and 110–140 km west and west-southwest of KLSX. The snow is reducing visibilities to 0.93 km (0.5 statute mi) at KSTL and Spirit of St. Louis Airport (KSUS) at this time. Smaller discrete banded structures within the larger band can be seen 150 km southeast of KLSX and over parts of far southern Illinois. Pockets of 35–40 dBZ are embedded within the smaller mesoscale bands, which persist through the next 60 min and continue to indicate the potential for relatively high snowfall rates. The smaller mesoscale bands identified earlier over northeastern Missouri and west-central Illinois persist through this time. Reflectivity magnitudes did not change during the preceding 60 min.

The large mesoscale band at 1158 UTC (Fig. 8) continues to propagate slowly eastward across eastern Missouri through southern Illinois. Many of the smaller discrete banded features seen earlier are not observed across east-central Missouri and southwest Illinois at this time. However, smaller pockets of higher reflectivity (exceeding 35 dBZ) persist within the larger band and still suggest the presence of relatively high snowfall rates. Snow continues to reduce visibilities to 0.93 km (0.5 statute mi) at KSTL and KSUS, making commuter travel very slow and difficult. The overall reflectivity pattern at this time also shows the development of a strong reflectivity gradient along the southern (trailing) side of the large mesoscale band during the preceding 60 min. This type of reflectivity pattern is absent along the southern flank of the precipitation band during the earlier periods, but noted along the forward edge of the mesoscale band during this time.

b. Wind profiler observations

The wind profiler at Winchester, Illinois (WNCI2), resides just north of the event site and reveals several features of the flow and its evolution throughout the event (Fig. 9). First, we note the persistent easterly flow depicted below 1000 m through 1500 UTC 10 April 1997. Our surface analysis has shown that the driest air lies east of the STL area (Fig. 3a), so that a supply of dry surface air was advecting into this region overnight. Next, we note the shift from easterly to westerly flow at ~850 mb between 0300 and 0800 UTC. In fact, winds are so light and variable with the ridge passage as to preclude measurable values between 0400 and 0700 UTC on 10 April 1997. Yet, this behavior, indeed the entire pattern, depicts clearly the passage of a ridge over the site from west to east.

This ridge motion, in conjunction with the wind profile evolution, provides the deformation needed to manipulate the thermal field with time. At 0200 UTC, a backing wind profile is shown in the 850–600-mb layer, suggesting cold advection east of the ridge axis. Later at 0900 UTC, a veering wind profile in the same layer allows us to infer warm advection west of the ridge axis. In total, this analysis suggests a pathway for dry air in the boundary layer, beneath ingredients for low- to midlevel frontogenesis, analyzed previously.

4. Model simulation

In order to better document the short-term changes in the thermodynamic profile that attended this event, solutions from a mesoscale numerical model are em-

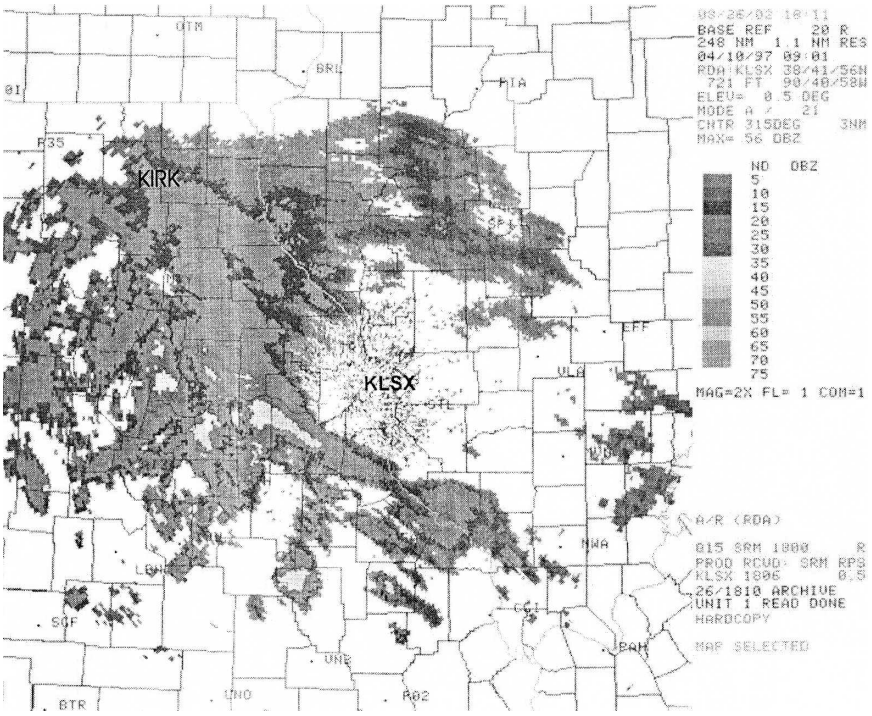

FIG. 5. St. Louis, MO (KLSX), WSR-88D plot of base reflectivity at the 0.5° elevation angle at 0901 UTC 10 Apr 1997.

ployed. In this case, such a model was being run daily in a real-time operational mode at Saint Louis University. Archived output from that simulation platform for the date in question are examined presently.

a. MASS configuration

The Mesoscale Atmospheric Simulation System (MASS), version 5.10.1, was used to model this system (e.g., Manobianco et al. 1996) in real time. Two grids from the archive are employed in this study (50 and 25 km) that featured one-way interaction, both initialized at 0000 UTC 10 April 1997 and run for 24 h. Lateral boundary conditions (LBCs) for the 50-km run (Fig. 10) are derived from the 80-km, 6-hourly grids from the Eta Model run initialized at the same time. The LBCs for the 25-km simulation (Fig. 10) are derived from the hourly output from the 50-km MASS run. Both simulations feature a hydrostatic atmosphere with 21 vertical levels formulated in terrain-following σ-coordinates. Cumulus closure is provided by the a Kuo–Anthes scheme (Kuo 1965; Anthes 1977) that has been modified to include moist downdrafts, while the planetary boundary layer is resolved with a 1½-order turbulent kinetic energy scheme (Therry and Lacerrère 1983; Benoit et al. 1989).

Explicit moisture physics account for mixed-phase precipitation, although without treatment for hail. The MASS prognostic moisture scheme includes expressions for the conservation of cloud water and cloud ice. The equation for the conservation of cloud water possesses a fallout term, which is integrated from the top of the model atmosphere to the bottom of the model's lowest layer. For temperatures less than 0°C in the presence of snow, fallout of snow is calculated assuming a particular snow size distribution and terminal fall speed (Zhang 1989).

b. Surface fields

The 25-km MASS integration depicts snow just beginning to accumulate by 1200 UTC 10 April 1997 in the St. Louis area (Fig. 11a), which corresponds rather well with the observations at KSTL (Table 1), although the modeled amounts lag behind the actual values. Actual snow accumulated to 2.5 cm (1 in.) between 1100 and 1200 UTC 10 April 1997, although snow had begun at 1019 UTC; approximately the first hour of snowfall had melted upon reaching the ground. The modeled amount at 1200 UTC at STL is less than 1.3 cm (0.5 in.).

By 1500 UTC, 10 cm (4 in.) of actual snow had fallen at KSTL, while the MASS value amounts to only 3.8 cm (1.5 in.; Fig. 11b). Also, the rate of eastward development of the modeled precipitation is slower. Yet, the

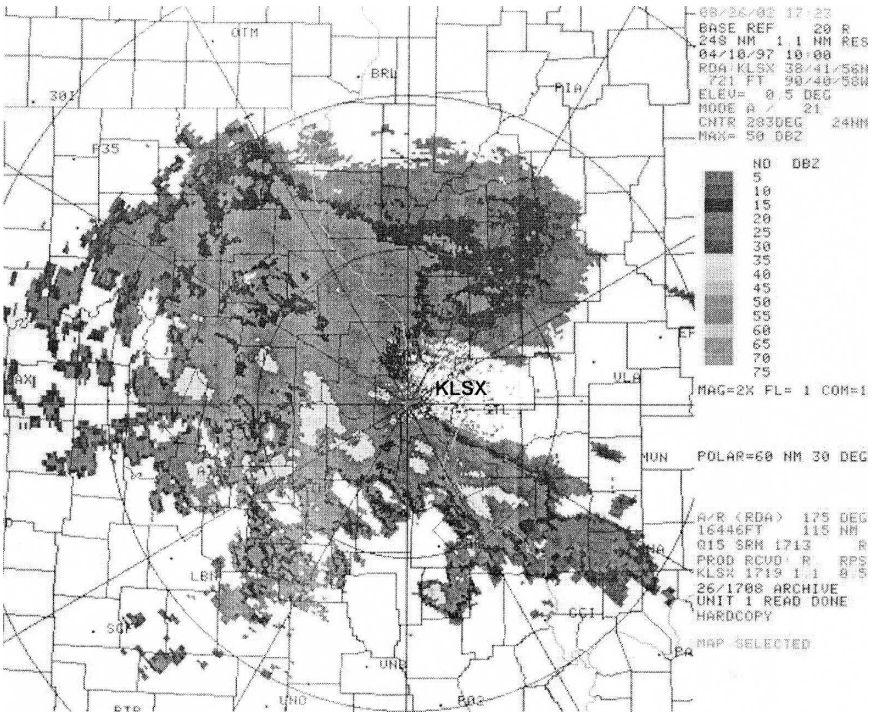

FIG. 6. As in Fig. 5 but for 1000 UTC 10 Apr 1997.

MASS solutions at both 1200 and 1500 UTC feature patterns that correspond well to the observed snow swath (see Fig. 1) as well as the radar observations of the event. Moreover, the timing of modeled snow onset in and around St. Louis and the remarkable qualitative agreement between the simulated snowband and that observed on radar at nearly the same time lends confidence to using the output in a diagnosis of this event.

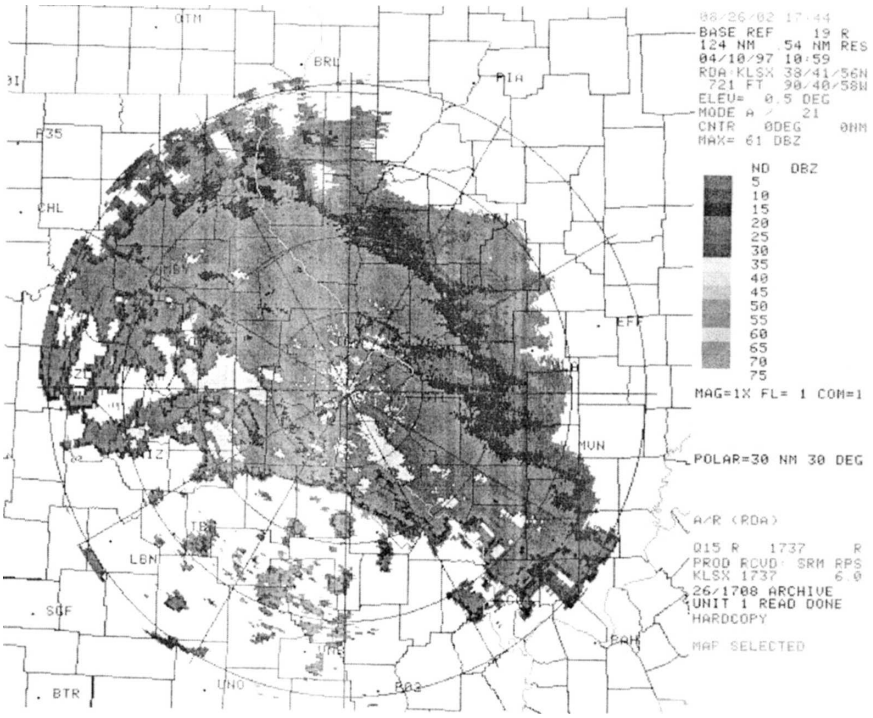

FIG. 7. As in Fig. 5 but for 1059 UTC 10 Apr 1997.

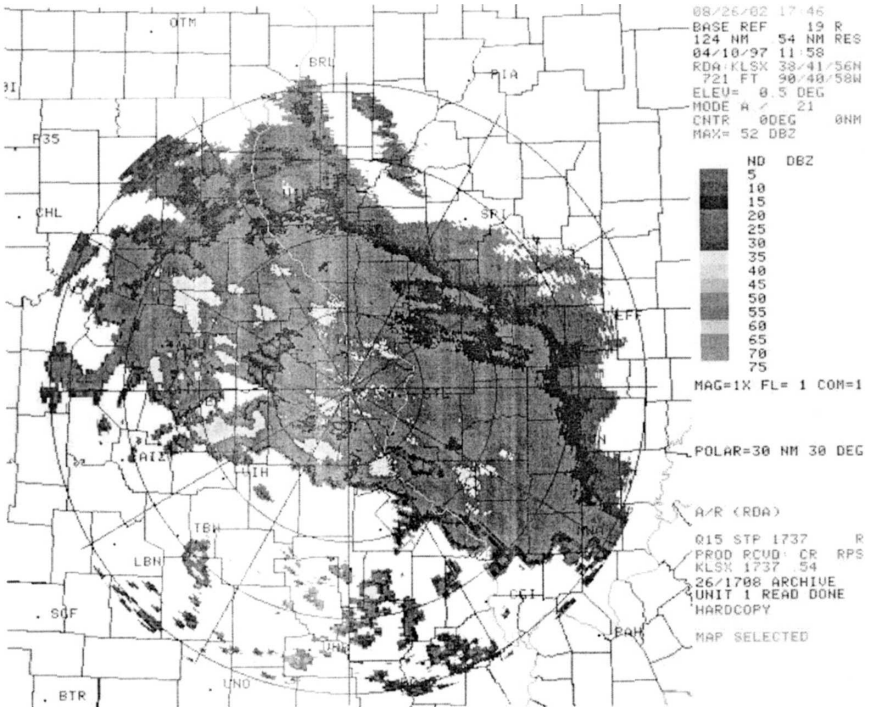

FIG. 8. As in Fig. 5 but for 1158 UTC 10 Apr 1997.

c. *Frontogenesis*

Given the low-level deformation zone associated with the elongated ridge axis, frontogenesis is explored as a forcing agent for ascent. While significant midtropospheric Q-vector convergence is found over the STL area at 1200 UTC on 10 April, the associated frontogenesis is also useful for the diagnosis of the low-level cooling associated with the evaporation and melting of falling snow.

Frontogenesis maximizes over St. Louis at 1000 UTC in the midtroposphere (near 700 mb), with values in excess of 3 K $(100\ \text{km})^{-1}$ $(3\ \text{hr})^{-1}$ (Fig. 12). This $\mathcal{F}$ maximum is associated with vertical velocity maxima farther aloft at 0900 UTC ($<-14\ \mu\text{b s}^{-1}$)and 1100 UTC ($<-16\ \mu\text{b s}^{-1}$). Thus, upward motion in the model is maximized up to 3 h before modeled snowfall begins to accumulate. This not only demonstrates the importance of $\mathcal{F}$ for the forcing for ascent, but also the 2–3-h delay between maximum forcing for ascent and the first simulated precipitation at the ground suggests the evaporation of falling precipitation near the ground.

Frontogenesis also persists at the 900-mb level beginning after 0400 UTC (Fig. 12), but becomes frontolytic between 1100 and 1200 UTC. Concurrently, at 900 mb over St. Louis, convergence is diagnosed at 0600 UTC and persists until at least 1200 UTC (not shown). Meanwhile, upward motion at 900 mb weakens between 1100 and 1200 UTC concurrent with the onset of frontolysis (Fig. 12), which is due to a change in sign in the resultant deformation term. Yet, the thermal gradient over eastern Missouri also relaxes by nearly a factor of 2 between 0900 UTC (Fig. 13a) and 1200 UTC (Fig. 13b). Additionally, the simulated 900-mb potential temperature field over KSTL at 1200 UTC was 281.5 K, which corresponds to an actual temperature of 273.1 K, which is of course the freezing temperature of liquid water. We will return to this point shortly.

d. *Sublimational cooling*

Cross-sectional analysis from model output valid at 0900 UTC (Fig. 14a) reveals the strongest $\mathcal{F} \sim 100$ km north of the St. Louis area at 700 mb [3 K $(100\ \text{km})^{-1}$ $(3\ \text{h})^{-1}$] beneath an upward vertical velocity maximum ($<-12\ \mu\text{b s}^{-1}$). This also concurs with the ascending branch of a weak direct thermal circulation (Fig. 14b). Notice the increased ageostrophic component with height over St. Louis, especially in the 900–700-mb layer. This shear profile plays a role in altering the stability (lapse rate) profile there. The strength of the ascent also produces a heating maximum at 500 mb as evidenced by the bowing of the isentropes downward toward the surface, increasing the stability beneath the $\mathcal{F}$ maximum.

The lower troposphere near St. Louis is also host to a weak and confined, but locally enhanced, region of $\mathcal{F}$ and upward motion beneath 850 mb at this time. We

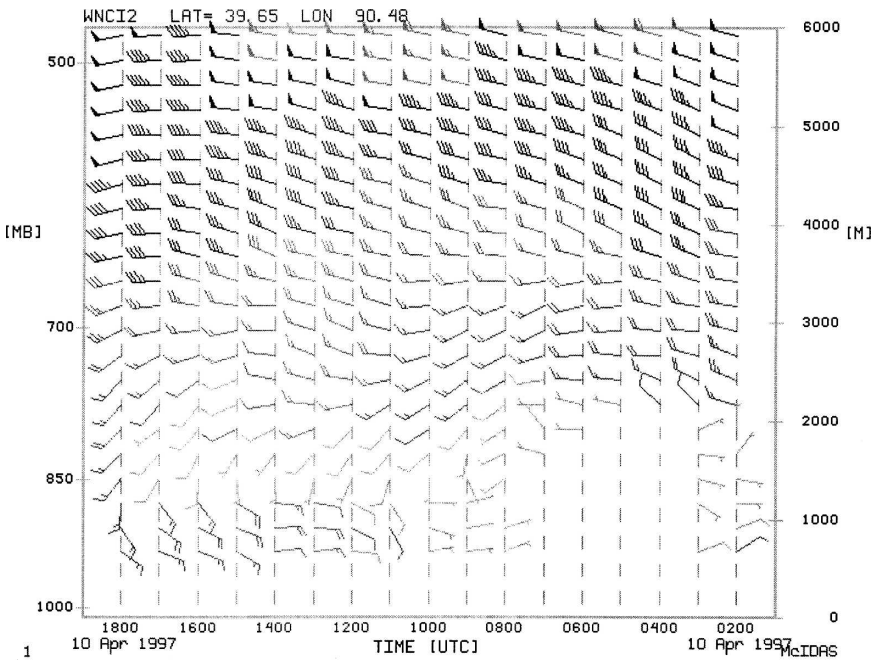

FIG. 9. Wind profiler data for the lower troposphere (every 250 m, up to 6000 m) over Winchester, IL, from 0200 to 1800 UTC 10 Apr 1997 (time increases from right to left). Shaft points in the direction of the horizontal flow; flags represent 50 kt, long barbs denote 10 kt, and short barbs denote 5 kt.

note, too, the weaker stability profile just south of St. Louis, with isentropes bowing upward slightly near the 850-mb level, in response to the precipitation falling into that region and sublimating (Fig. 14b). This cooling, coupled with the confluent flow in and around that layer, acts to compress the thermal gradient, thereby enhancing $\mathcal{F}$, especially south of KSTL.

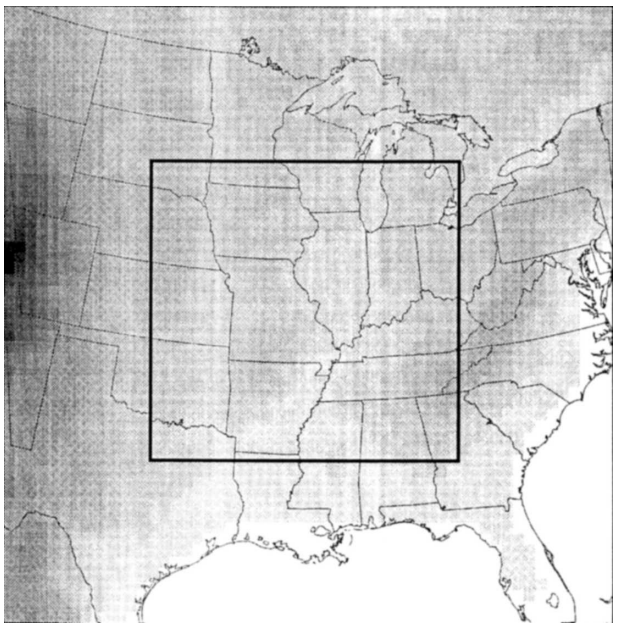

FIG. 10. The 50- (outer box) and 25-km (inner box) domains for MASS model simulations. Shading denotes elevation, with the darkest/highest locations (3300 m) on the western boundary.

At 1200 UTC, both $\mathcal{F}$ and the vertical velocities are weaker in the midtroposphere (Fig. 15). Nearer the surface, descent (similar to that described by Parker and Thorpe 1995) and diffluence are diagnosed over St. Louis, with a horizontal roll structure south of St. Louis. A region of weaker static stability is found there concurrent with the strongest upward vertical velocity near the surface and a sloping region of $\mathcal{F}$ similar to that at 0900 UTC (Fig. 14a), yet more pronounced, with maxima persisting on the lower northern side and upper southern side of the stability minimum. This behavior is consistent with precipitation falling into a dry layer and sublimating, thus cooling the lower environment and inducing the region of weaker static stability adjacent. It is clear that the local changes in $\mathcal{F}$ are more the result of changes in the θ gradient, which respond *immediately* to diabatic heating–cooling and less due to changes in the wind field, which respond over time to such thermal changes via the mass field. Thus, we speculate that a kind of baroclinicity is present here similar to that documented by Szeto and Stewart (1997), with the sublimation-cooled downdraft residing below and north of the ascent and greatest warming. This process would help account for the migration of

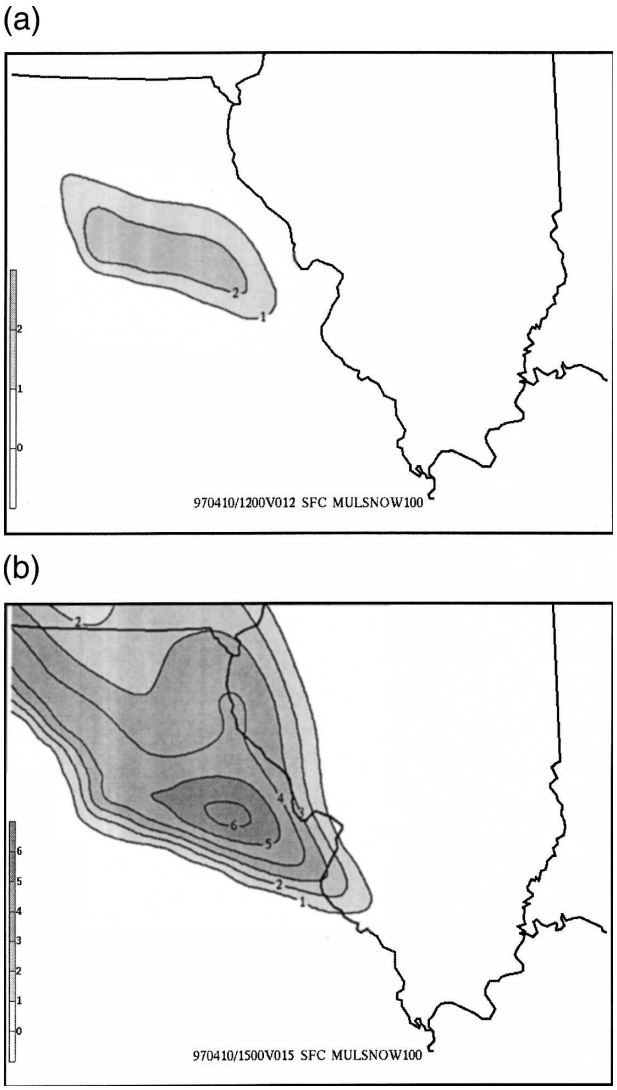

FIG. 11. MASS-simulated snowfall totals (cm) valid at (a) 0900 and (b) 1200 UTC 10 Apr 1997.

the strongest radar echoes to the south side of the actual mesoscale band as discussed in the text in section 3a.

The modeled lapse rate tendency is examined for the lower troposphere over Missouri using the lapse rate tendency equation developed and discussed at length by the Air Force Weather Agency (AWS 1979) and given as

$$\frac{\partial \gamma}{\partial t} = \underbrace{-\frac{1}{c_p}\frac{\partial}{\partial z}\left(\frac{dQ}{dt}\right)}_{\text{A}} \underbrace{- \mathbf{V}\cdot\boldsymbol{\nabla}\gamma}_{\text{B}} + \underbrace{\frac{\partial \mathbf{V}}{\partial z}\cdot\boldsymbol{\nabla}T}_{\text{C}} + \underbrace{\frac{\partial w}{\partial z}(\Gamma - \gamma)}_{\text{D}} \underbrace{- w\frac{\partial \gamma}{\partial z}}_{\text{E}}. \quad (2)$$

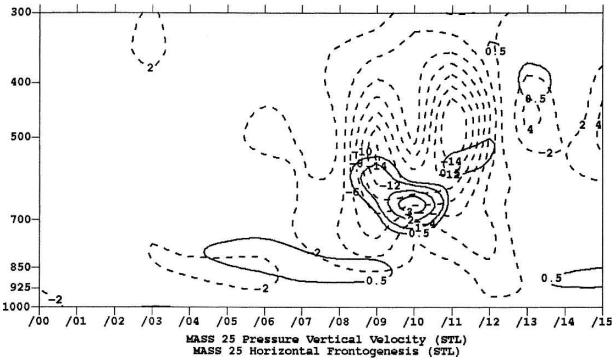

FIG. 12. Time–height section for St. Louis, MO, of vertical velocity (dashed; every 2 μb s^{-1}) and frontogenesis [solid; contoured at 0.5, 1, 2, and 3 K (100 km)$^{-1}$ (3 h)$^{-1}$].

Assuming that sublimation of snow is cooling progressively lower levels of the atmosphere, this expression is employed so that we may quantify the processes that affected the near-surface lapse rate. In this expression, $\gamma = -\partial T/\partial z$ such that negative values in any of the terms indicate increasing stability in the chosen layer. Term A describes the vertical variation of diabatic heating in a column, term B describes the horizontal advection of lapse rate through a column, term C accounts for vertical wind shear and thus different rates of ageostrophic advection at different levels that can affect a change in static stability, term D requires stabilization (destabilization) for a shrinking (stretching) column, and term E represents the vertical advection of lapse rate.

In this case, we calculate all terms from the model solution (including the left-hand side) except diabatic heating (term A), for which we solve as a residual. This is done for several reasons. First and foremost, diabatic heating was not included as output in the archived model fields when the simulation was run in real time. Second, and in league with the first, operational model output readily available to field forecasters still lacks any representation of diabatic heating. Meanwhile, all other terms in (2) are readily calculable, and the process undertaken here is easily repeatable. As for the error included in the residual term, our calculations following the approach of Moore (1985) suggest that it amounts to no more than 10% of the total value of the diabatic heating term.

Average values for each term are calculated from the four model grid points around STL. The lapse rate tendency in the 1000–3000-m layer is a simple subtraction of the actual lapse rate γ at 0900 UTC from the value at 1200 UTC, while the remaining terms are averaged over the 3-h period. The lapse rate advection term (term B) is computed at 2000 m while term C employs

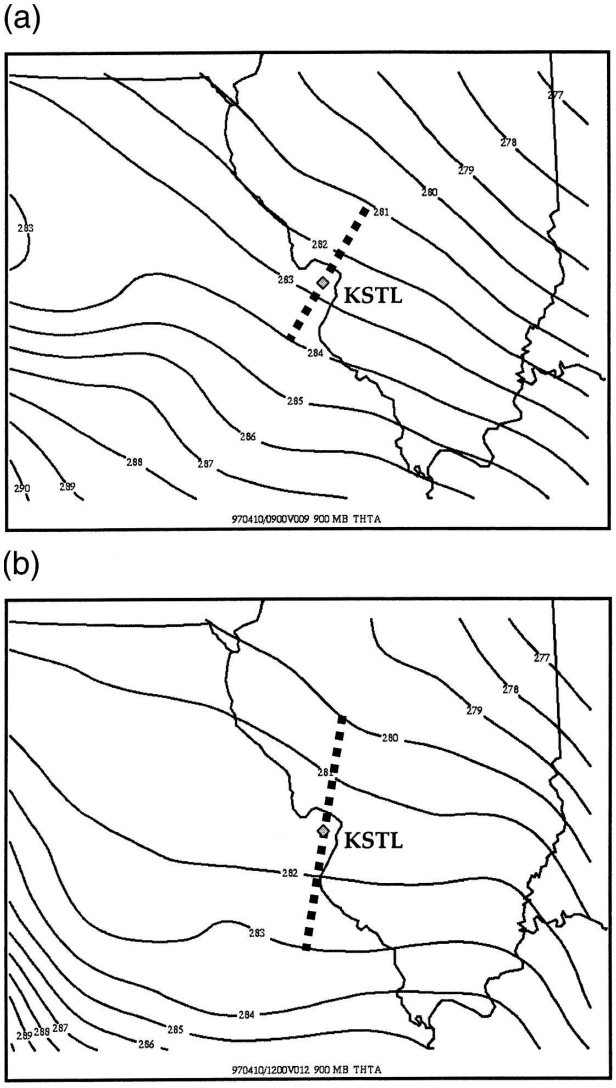

FIG. 13. Plan view analysis of model-predicted potential temperature (K) at 900 mb valid at (a) 0900 and (b) 1200 UTC 10 Apr 1997. The diamond is centered on KSTL. The dashed bars are provided to show the change in distance with time between the 280- and 283-K isentropes.

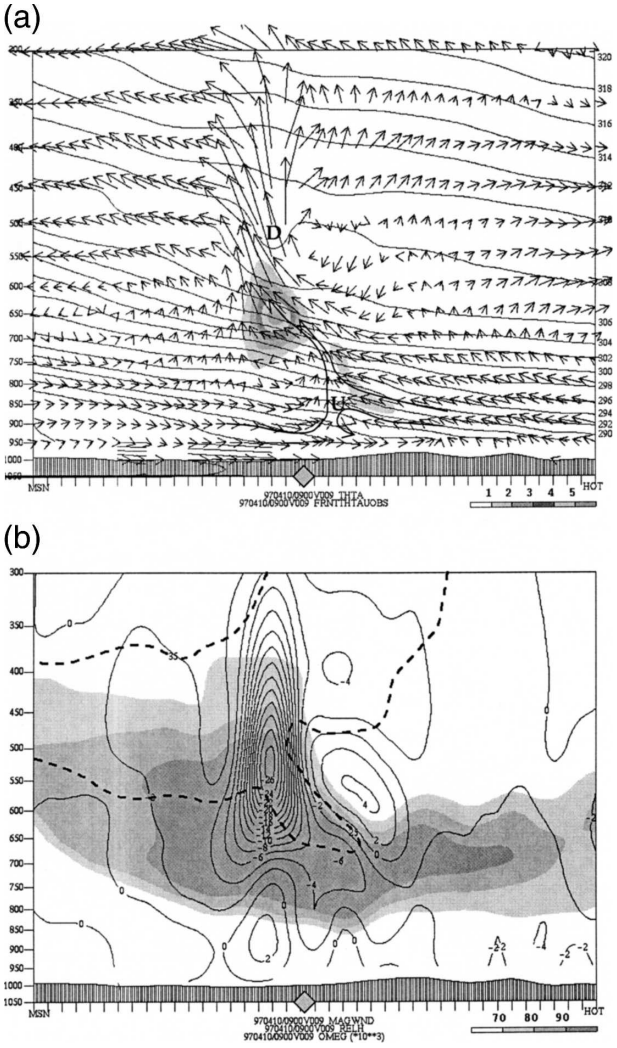

FIG. 14. Cross sections from Madison, WI (MSN), to Hot Springs, AR (HOT), of model output valid at 0900 UTC 10 Apr 1997 depicting (a) potential temperature (solid, every 2 K), frontogenesis [shaded, every 1 K $(100\ \text{km})^{-1}\ (3\ \text{h})^{-1}$], and circulation vectors (with selected subjective streamlines, the sum of the horizontal ageostrophic wind in the plane of the cross section and ω, both of which have been scaled to the cross section), and (b) ω (solid, every 2 μb s^{-1}), relative humidity (shaded above 70%), and isotachs (dashed, 25 and 35 m s^{-1}). Diamond near the bottom-middle of the figure is the location of the St. Louis, Missouri, metropolitan area. The boldface D and U in (a) define regions of downward and upward isentrope bowing, respectively.

a shear over the 1000–3000-m layer depth with a temperature gradient at 2000 m. Term D is evaluated with vertical velocities and stability in the 1000–3000-m layer, and term E is calculated with vertical motion at 2000 m and lapse rates in the 1000–2000- and 2000–3000-m layers. Ultimately, time averaging makes these values valid over STL in the 1000–3000-m layer at 1030 UTC 10 April 1997.

Term values calculated for (2) are listed in Table 2. Stability increases between 0900 UTC (Fig. 16a) and 1200 UTC (Fig. 16b) as indicated by the negative tendency of $\partial\gamma/\partial t$. This is obvious in the skew T–log$p$ analyses with cooling at 1000 m by 1200 UTC (Fig. 16b), while the temperature at 3000 m is unchanged during the period. All of the remaining terms are negative also, except for advection, which depicts the encroachment of a less stable lapse rate in that layer. Although large, the advection is nearly offset by the shear term (term C), which suggests an ageostrophic vertical circulation in that layer. We have seen evidence of this occurring near the surface (Fig. 14a). Terms D and E are one to

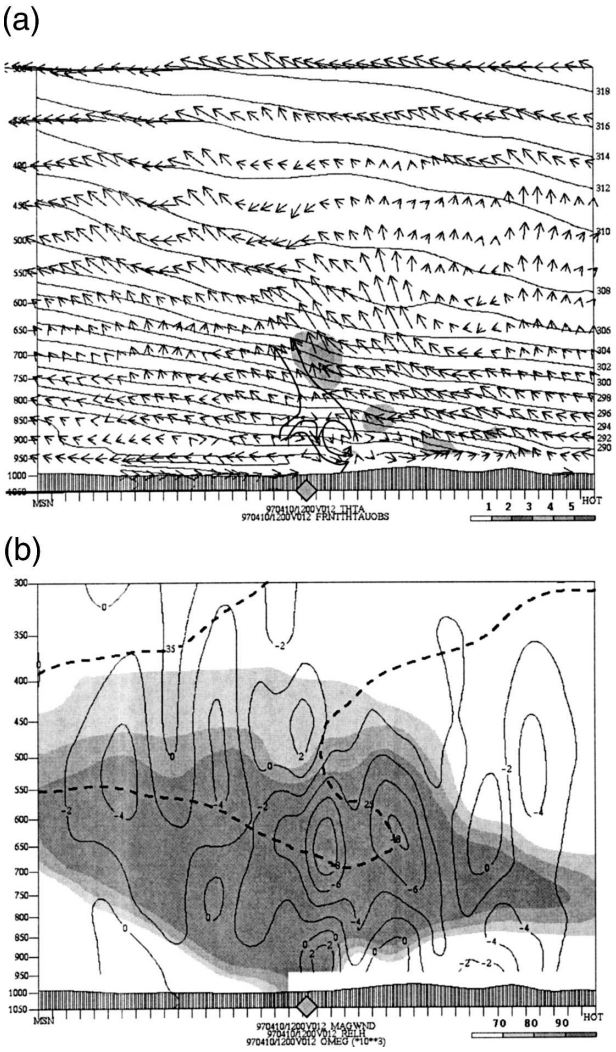

FIG. 15. As in Fig. 14, but with output valid at 1200 UTC 10 Apr 1997

two orders of magnitude smaller, respectively, than terms B and C. However, they both indicate increasing stability. With term D, we have a situation where the top of the column is ascending more slowly than the bottom. The result is less cooling aloft and increased stability. With term E, the upward vertical motion is acting to transport greater stability upward. This is particularly true between 1000 and 3000 m at 0900 UTC as evidenced by the nearly isothermal layer around 850 mb in Fig. 16a.

Returning to term A, we find a negative value in Table 2, which indicates stabilization. The reason for this behavior is the latent heat release occurring near the top of the layer (~3000 m) and the cooling of the atmosphere as precipitation particles sublimate at the base of the layer (~1000 m). We can visualize the moistening and cooling processes by examining model time sections for KSTL (Fig. 17). Rapid moistening occurs below 850 mb between 1000 and 1200 UTC (Fig. 17) and does so from the top down. The 0°C isotherm descends from the ~825 mb level to very near the surface by 1400 UTC, lagging the actual observation of 0°C at KSTL at 1100 UTC (Table 1). In fact, this modeled rate is slower than the observed time frame of Wexler et al. (1954). By 1200 UTC, the MASS has generated a more stable, nearly isothermal layer over KSTL from the surface to ~800 mb. With the other terms in control of the lapse rate tendency nearly offsetting, the vertical change in diabatic heating dominates the near-surface temperature profile (Table 2). This is most striking at 1000 UTC (Fig. 17) with warming over KSTL in the 800–650-mb layer while slower cooling persists nearer the surface. A simple estimate of the latent heating field following Cammas et al. (1994) from the MASS solutions reveals weak cooling by 1200 UTC over STL at 900 mb (Fig. 18b). Note also that the region of strongest cooling is nearly coincident with the region of greatest simulated 3-h snowfall (Fig. 11).

We note that a broad region at the surface was conducive to such cooling. Even at model initialization, some 10 (11) h before the beginning of actual (modeled) snowfall at the surface, T_i in the −1°C to +1°C range cover the northern half of Missouri with dewpoint depressions >10°C over most of the state (Fig. 19). This surface wet-bulb field is a pattern that features values well below the upper threshold for snow of Lumb (1961) and evolves little over the ensuing 9–12 h. Using the surface T_i in concert with the surface dewpoint depression is an excellent combination for defining the threat area in hindsight. Although data on the situation aloft are always helpful, these two parameters yield a measure of how dry the surface air is and what actual temperature one will likely have if that dry surface layer is moistened completely by sublimation.

To be certain that the melting of snow was not a significant factor in determining precipitation type at STL, both observations and model solutions upstream of STL were examined. Observations from Belleville, Illinois (BLV), which is upstream of STL [for easterly flow in the planetary boundary layer (PBL)] began as snow and persisted that way well into the morning (1700 UTC). Likewise, observations from Rolla, Missouri (VIH), which is also upstream of STL (for the west-southwesterly flow above the PBL), reported no snow. Due west of STL at Columbia, Missouri, precipitation began as snow and lasted that way until after sunrise (1300 UTC). Similar to the St. Louis observations (Table 1), temperatures at BLV are 3°–4°C at snow onset, but rapidly cool and moisten in under an

TABLE 2. Terms in the lapse rate tendency equation valid at 1030 UTC 10 Apr 1997 in the 1000–3000-m layer over St. Louis, MO. Each term is expressed in units of 10^{-7} K m^{-1} s^{-1}. All terms are calculated from the model solutions except the diabatic heating term for which we solved as a residual.

$(\partial\gamma/\partial t)$	$-(1/c_p)(\partial/\partial z)(dQ/dt)$	$-\mathbf{V}\cdot\nabla\gamma$	$(\partial\mathbf{V}/\partial z)\cdot\nabla T$	$(\partial w/\partial z)(\Gamma-\gamma)$	$-w(\partial\gamma/\partial z)$
−0.579	−0.635	+0.650	−0.563	−0.028	−0.004

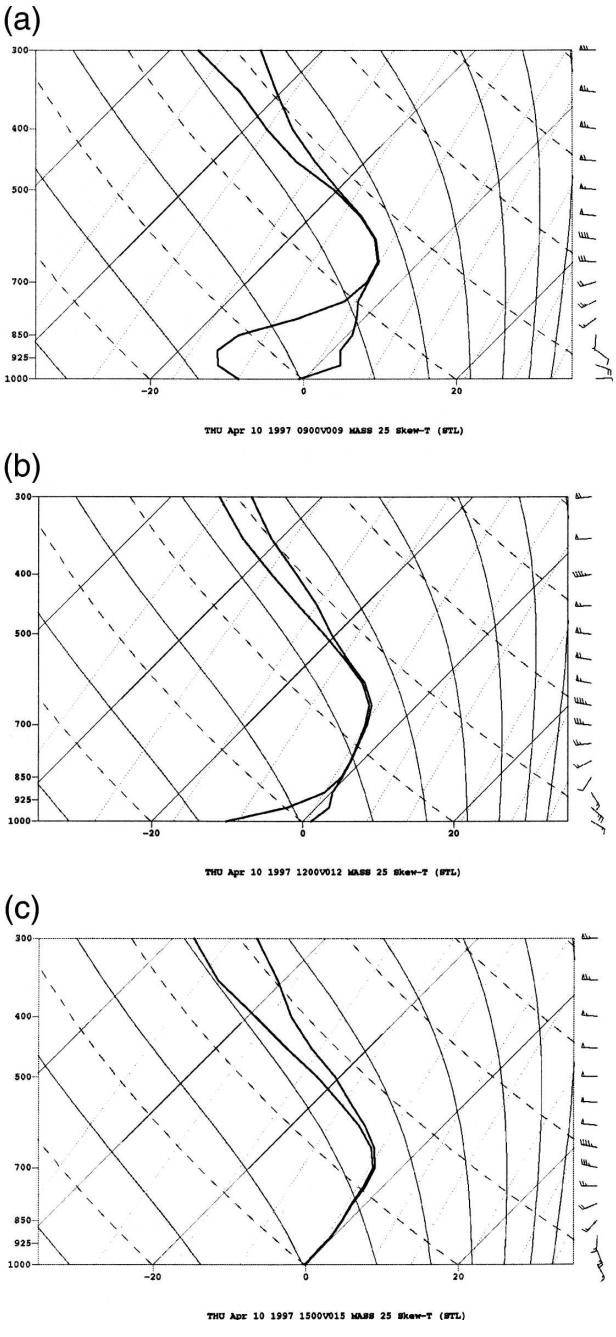

FIG. 16. Model-predicted skew T–log$p$ analyses for KSTL showing standard T and T_d profiles, with wind profile (kt) on the right-hand side. Analyses are valid at (a) 0900, (b) 1200, and (c) 1500 UTC 10 Apr 1997.

hour. Thus, there is some melting in the area, but it is short lived. Given that the latent heat of melting is significantly less than the latent heat of evaporation, the latter is dominant in this case. This assertion is supported by the MASS soundings from BLV, which reveal a nearly isothermal wet bulb temperature of −2°C to −3°C in the lowest 150 mb, not unlike the 1200 UTC observed ILX sounding (Fig. 4e). Moreover, the MASS depicts a similar progression over VIH. At 0900 UTC in a layer over VIH from 800 to 700 mb, the temperatures and dewpoints are both above 0°C. Otherwise, the wet-bulb profile remains below 0°C. Indeed, the radar signatures suggest melting at that time, although none of the surface observations of precipitation support this idea. Yet, given the MASS solutions for that location (VIH) and time, it seems likely that melting did drive up the reflectivities aloft, southwest of STL (e.g., Fig. 5).

5. Conclusions

This paper examines a case of surprise, late-season snowfall in the midwest United States, wherein cooling through the sublimation of falling snow was the key to determining precipitation type. During the observed event, rain was not reported initially at the surface stations studied, and the evolution of the hourly soundings for KSTL depicted moistening from the top down and

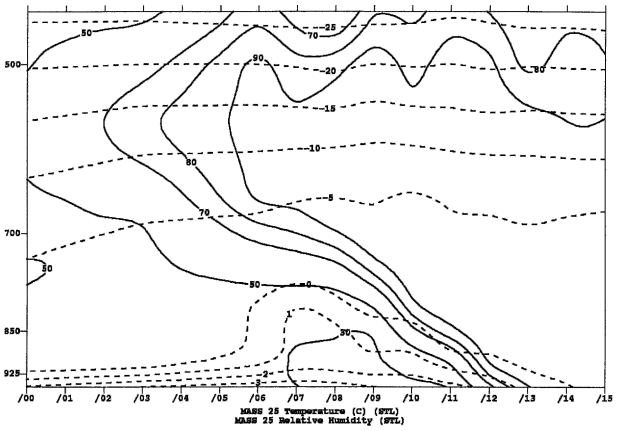

FIG. 17. Model-predicted time–height section for KSTL from 0600 to 1500 UTC 10 Apr 1997 showing relative humidity (solid, every 10%) and temperature (dashed, every 5°C up to 0°C).

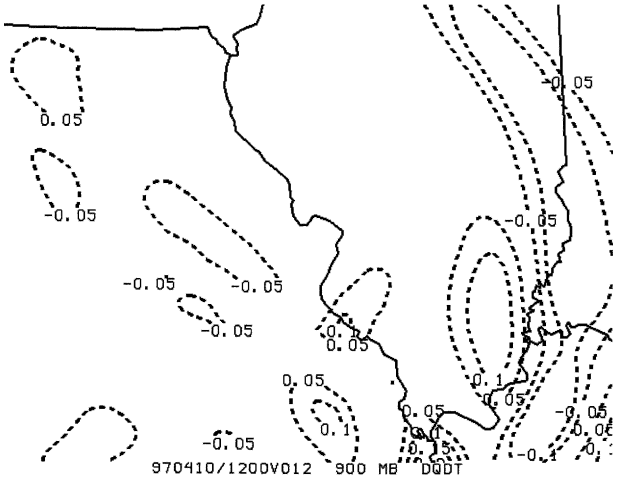

FIG. 18. Diabatic heating (dashed; every 0.05 K s^{-1}) at 900 mb from MASS 12-h solutions valid at 1200 UTC 10 Apr 1997.

nearly isothermal wet-bulb temperature profiles at about 0°C throughout a deep layer. Yet, while the dominant process here was not melting, parallels may be drawn between this work and recent literature on the melting process.

In particular, our findings in this study concur with the forecast guidelines set forth by Kain et al. (2000) for the anticipation of melting-induced snow. Low-level temperature advection in this case was weak. It is true that the contribution of thermal advection in the lapse rate tendency equation was significant at 1030 UTC (Table 2). However, it was not only compensated for by competing terms, but also was valid at a height of 2000 m. Examination of Fig. 3a supports the assertion that near-surface thermal advection was indeed weak. The flow was northeasterly at KSTL, in the weak outward spiraling flow about the synoptic-scale anticyclone.

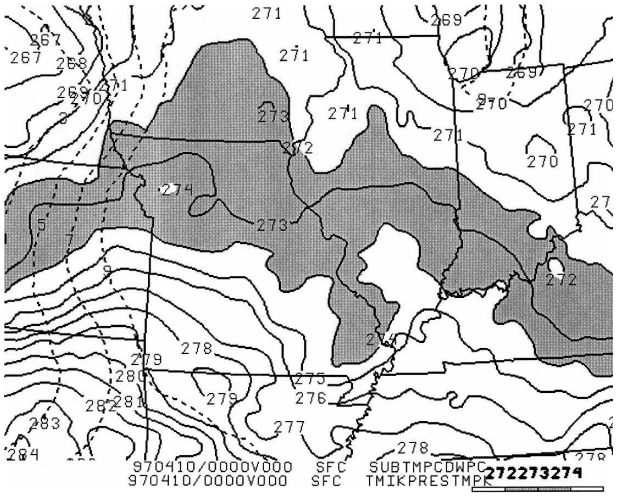

FIG. 19. Plan view analysis of model-predicted dewpoint depression (dashed at 3°, 5°, 7°, and 9°C) and ice-bulb temperature (shaded between −1°C and +1°C, with the attendant isotherms as well as that for 0°C shown as solid contours) valid at 0000 UTC 10 Apr 1997.

Second, temperatures in KSTL were within 3°C of freezing at the onset of the event (Table 1). However, the dewpoint was also −4°C, such that further cooling through evaporation/sublimation was inevitable. Indeed, it was the depth of the layer of dry air over KSTL with a $T_w = 0$°C that forced this event to deviate from the Kain et al. (2000) model.

Their third forecasting guideline was that steady-state rainfall of at least moderate intensity should be expected for several hours. In letter and in spirit, that was the consensus forecast heading into the morning of 10 April 1997. However, the depth of the dry air near the surface eliminated the possibility of rain in the KSTL area, and precipitation began and lasted for several hours as snow before changing over to rain.

Clues to the dominance of sublimational cooling come from the surface T_i field and the surface dewpoint depression analysis (Fig. 19). This analysis reveals cooling due to sublimation, with the target temperature of 0°C. The influence of this top-down cooling was relatively local, especially in the presence of weak surface thermal and moisture advections. Note that sublimational cooling was dominant in this case, which is further supported by the behavior in the simulated skew T–log$p$ diagrams over KSTL (Fig. 16). Much like the zipper door of a camping tent, the temperature and dewpoint temperature profiles come together at the top of the evaporation layer and, later, closer to the surface. Although an isothermal layer near 0°C was created near the surface, the primary cause in this case was esublimational cooling, with melting becoming more significant (but still minor) toward the end of the event.

The discriminator between these classes of events seems to be the T_w profile in the near-surface layer. For cases wherein melting is the dominant force for the creation of snowfall, it is beneficial for the T_w profile to be above freezing initially. This allows saturation due to evaporation/sublimation to occur first at a temperature above freezing, followed by additional cooling via melting. These events begin as rain, and involve a subsequent change to snow. The event studied here exhibited an initial T_w profile that was nearly isothermal and very nearly 0°C. As a consequence, and in concert with the initially dry layer near the surface, sublimation cooled and moistened the environment to saturation, with a resulting near-surface layer ambient air temperature of 0°C.

In closing, it is unlikely that forecasters would miss such an event again. Technological advances and soft-

ware that permit easy manipulation of model guidance have emerged on the operational scene since this event occurred. Plots of soundings (including T_w) and their evolution (loops and time-height sections) are now a simple matter to produce in real-time. Such resources should make it less likely for forecasters to overlook the possibility of a snow event in this type of environment.

Acknowledgments. We begin by thanking Dr. John Zack of MESO, Inc., for making the code for the MASS model available to us. The authors also thank Dr. James T. Moore for his encouragement of this study in its early stages; additionally we express our gratitude to Dr. Glenn Van Knowe for his technical expertise with running the MASS and Dr. Charles Graves for assistance with the postprocessing. We are also grateful to Steve Chiswell for his help with incorporating new code into GEMPAK and to Chris Melick for his assistance in drafting some figures. Finally, the comments of Dr. John Kain and several anonymous reviewers have vastly improved the final manuscript.

REFERENCES

Anthes, R. A., 1977: A cumulus parameterization scheme utilizing a one-dimensional cloud model. *Mon. Wea. Rev.,* **105,** 270–286.

AWS, 1979: The use of the skew T, log P diagram in analysis and forecasting (revised 1995). Air Weather Service Rep. AWS/TR-79/006, Air Weather Service, Scott Air Force Base, IL, 164 pp.

Benoit, R., J. Côté, and J. Mailhot, 1989: Inclusion of a TKE boundary layer parameterization in the Canadian Regional Finite-Element model. *Mon. Wea. Rev.,* **117,** 1726–1750.

Cammas, J. P., D. Keyser, G. M. Lackmann, and J. Molinari, 1994: Diabatic redistribution of potential vorticity accompanying the development of an outflow jet within a strong extratropical cyclone. *Proc. Int. Symp. on the Life Cycles of Extratropical Cyclones,* Vol. III, Bergen, Norway, Geophysical Institute, University of Bergen, 403–409.

Gedzelman, S. D., and E. Lewis, 1990: Warm snowstorms: A forecaster's dilemma. *Weatherwise,* **43** (5), 265–270.

Hansson, M., 1999: A study of the sub-cloud layer conditions during precipitation and at temperatures near freezing. Rep. DM 82, Dept. of Meteorology, University of Stockholm, Stockholm, Sweden, 43 pp. [Available from Library, Dept. of Meteorology, Stockholm University, Arrhenius Laboratory, S-106 91 Stockholm, Sweden.]

Hess, S., 1959: *Introduction to Theoretical Meteorology*. R. E. Krieger Publishing, 364 pp.

Kain, J. S., S. M. Goss, and M. E. Baldwin, 2000: The melting effect as a factor in precipitation-type forecasting. *Wea. Forecasting,* **15,** 700–714.

Kuo, H. L., 1965: On formation and intensification of tropical cyclones through latent heat release by cumulus convection. *J. Atmos. Sci.,* **22,** 40–63.

Lumb, F. E., 1961: The problem of forecasting the downward penetration of snow. *Meteor. Mag.,* **90,** 310–319.

Manobianco, J., J. W. Zack, and G. E. Taylor, 1996: Workstation-based real-time mesoscale modeling designed for weather support to operations at the Kennedy Space Center and Cape Canaveral Air Station. *Bull. Amer. Meteor. Soc.,* **77,** 653–672.

McGuire, J., and S. Penn, 1953: Why did it snow in Boston in April? *Weatherwise,* **6** (6), 78–81.

Moore, J. T., 1985: A case study of the effects of random errors in rawinsonde data on computations of ageostrophic winds. *Mon. Wea. Rev.,* **113,** 1633–1643.

Nicosia, D. J., and R. H. Grumm, 1999: Mesoscale band formation in three major northeastern United States snowstorms. *Wea. Forecasting,* **14,** 346–368.

Novak, D. R., L. F. Bosart, D. Keyser, and J. S. Waldstreicher, 2002: A climatological and composite study of cold season banded precipitation in the northeast United States. Preprints, *19th Conf. on Weather Analysis and Forecasting,* San Antonio, TX, Amer. Meteor. Soc., 164–167.

Parker, D. J., and A. J. Thorpe, 1995: The role of snow sublimation in frontogenesis. *Quart. J. Roy. Meteor. Soc.,* **121,** 763–782.

Petterssen, S., 1956: *Weather Analysis and Forecasting*. Vol. 1. McGraw-Hill, 428 pp.

Szeto, K. K., and R. E. Stewart, 1997: Effects of melting on frontogenesis. *J. Atmos. Sci.,* **54,** 689–702.

Therry, G., and P. Lacerrère, 1983: Improving the eddy kinetic energy model for planetary boundary layer description. *Bound.-Layer Meteor.,* **25,** 63–88.

Wexler, R., R. J. Reed, and J. Honig, 1954: Atmospheric cooling by melting snow. *Bull. Amer. Meteor. Soc.,* **35,** 48–51.

Zhang, D.-L., 1989: The effect of parameterized ice microphysics on the simulation of vortex circulation with a mesoscale hydrostatic model. *Tellus,* **41A,** 132–147.